eISSN 2005-5447
International Journal of Stem Cells Vol. 16, No. 4, 2023 https://doi.org/10.15283/ijsc23045

REVIEW ARTICLE

In Vivo Stem Cell Imaging Principles and Applications

Seongje Hong[1], Dong-Sung Lee[2], Geun-Woo Bae[1], Juhyeong Jeon[1], Hak Kyun Kim[3], Siyeon Rhee[4], Kyung Oh Jung[1]

[1]*Department of Anatomy, College of Medicine, Chung-Ang University, Seoul, Korea,*
[2]*Department of Life Sciences, University of Seoul, Seoul, Korea,*
[3]*Department of Life Science, Chung-Ang University, Seoul, Korea,*
[4]*Stanford Cardiovascular Institute, Stanford University School of Medicine, Stanford, CA, USA*

Stem cells are the foundational cells for every organ and tissue in our body. Cell-based therapeutics using stem cells in regenerative medicine have received attracting attention as a possible treatment for various diseases caused by congenital defects. Stem cells such as induced pluripotent stem cells (iPSCs) as well as embryonic stem cells (ESCs), mesenchymal stem cells (MSCs), and neuroprogenitors stem cells (NSCs) have recently been studied in various ways as a cell-based therapeutic agent. When various stem cells are transplanted into a living body, they can differentiate and perform complex functions. For stem cell transplantation, it is essential to determine the suitability of the stem cell-based treatment by evaluating the origin of stem, the route of administration, *in vivo* bio-distribution, transplanted cell survival, function, and mobility. Currently, these various stem cells are being imaged *in vivo* through various molecular imaging methods. Various imaging modalities such as optical imaging, magnetic resonance imaging (MRI), ultrasound (US), positron emission tomography (PET), and single-photon emission computed tomography (SPECT) have been introduced for the application of various stem cell imaging. In this review, we discuss the principles and recent advances of *in vivo* molecular imaging for application of stem cell research.

Keywords: Stem cells, *In vivo* molecular imaging, Optical imaging, Magnetic resonance imaging, Positron emission tomography, Single-photon emission computed tomography

Introduction

In order to alleviate various chronic diseases, recent research are being conducted with transplanting sophisticated biomaterial scaffolds or transplanting organs. However, these various ways could induce an immune response and require immunosuppressive drugs after transplantation (1). In contrast, the regeneration of specific tissues and organs using stem cells could reduce the risk of side effects due to non-immune responses after transplantation. Stem cells have recently been studied in various ways as a cell-based therapeutic agent. Attention is focused on the treatment of diseases and body regeneration using induced pluripotent stem cells (iPSCs) as well as embryonic stem cells (ESCs), mesenchymal stem cells (MSCs), and neuroprogenitors stem cells (NSCs). Stem cell is being studied as a strategy to regenerate tissues and organs damaged by congenital defects and diseases (2). An advantage of stem cell regenerative medicine is that stem cell-based therapies do not require systemic immunosuppression unlike other regenerative approaches (3-5). The degree of symptom alleviation in diseases varies according to the amount of transplanted stem cells *in vivo* (6). For stem cell transplantation, it is essential to determine the suitability of

Received: April 15, 2023, Revised: July 13, 2023,
Accepted: July 21, 2023, Published online: August 30, 2023
Correspondence to **Kyung Oh Jung**
Department of Anatomy, College of Medicine, Chung-Ang University, 84 Heukseok-ro, Dongjak-gu, Seoul 06974, Korea
E-mail: kojung@cau.ac.kr

the stem cell-based treatment by evaluating the origin of stem, the route of administration, *in vivo* bio-distribution, transplanted cell survival, function, and mobility. Their effects and safety of stem cell would be enhanced by monitoring the accumulation of transplanted cells and long-term viability in target tissue. Moreover, assessing their function and toxicity *in vivo* could be achieved using various imaging modalities for applying cell-based therapeutics with promising preclinical results to clinical practices (7).

In vivo cell and molecular imaging is the visualization, characterization, and quantification of biological processes in humans and other living systems. *In vivo* molecular imaging could be used to determine the presence or absence of a disease and monitor the treatment of a disease (8-10). Various molecular images such as optical imaging, magnetic resonance imaging (MRI), positron emission tomography (PET), single-photon emission computed tomography (SPECT), and computed tomography (CT) allow us to visualize cellular and molecular processes with various genetic, metabolic, proteomic, and cellular biologic information. Comparing *in vitro* or *ex vivo* imaging, *in vivo* molecular imaging has many advantages to monitor the transplanted cells non-invasively in real time on an animal model. Especially, the unique characteristics and differentiation of the transplanted stem cells could be imaged through molecular imaging in the body. Currently, various stem cells are being imaged *in vivo* through various cell imaging methods (11-13). In this review, direct cell labeling methods using probes incorporated into cells or probes bound to cell membranes and indirect cell labeling methods that require genetic modification and image specific cells *in vivo* through an expressed reporter protein are described (Fig. 1). In addition, the basic principles of *in vivo* stem cell imaging are covered, the advantages and disadvantages of *in vivo* imaging methods, the latest research through *in vivo* stem cell imaging, and future research prospects are discussed.

Direct Cell Labeling Methods

Direct cell labeling methods are simple cell tracking methods that label specific target cells *ex vivo/in vitro* with a direct labeling agent and then inject and image *in vivo* (Fig. 2). *In vivo* cell imaging shows contrast agent-labeled

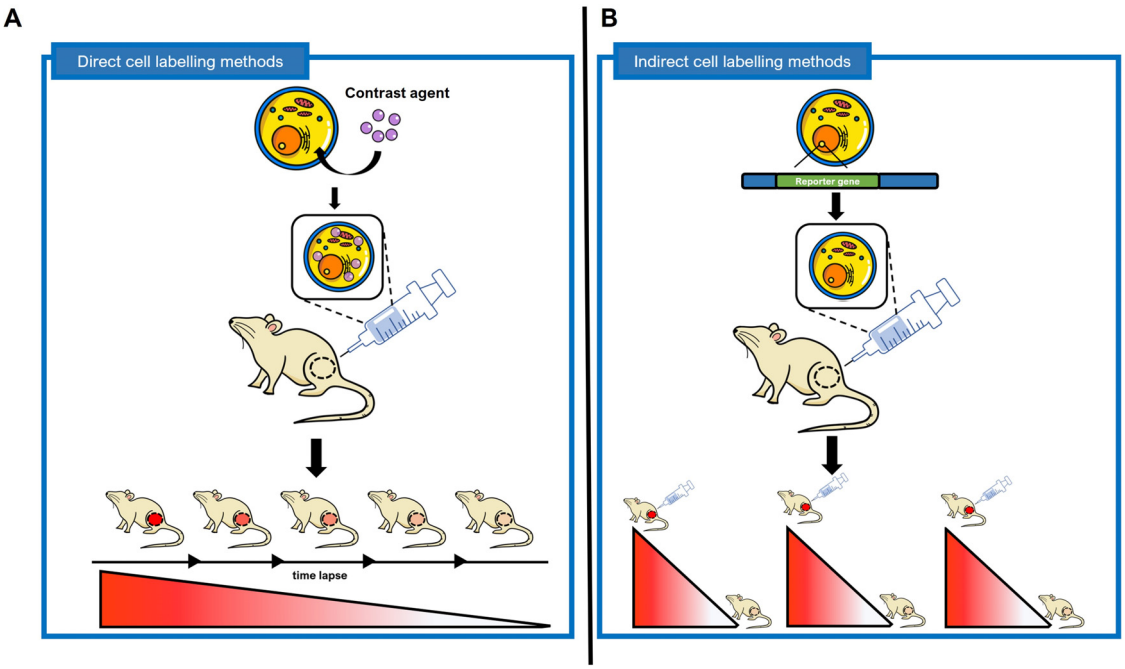

Fig. 1. Difference between direct cell labeling and indirect cell labeling. (A) Direct cell labeling methods are non-permanent imaging methods that identify direct labeling agents such as fluorescent dyes, superparamagnetic iron oxide nanoparticles, and isotopes labeled on cells *in vivo*. Direct labeling agent after labeled stem cells can be detected for several hours to several days depending on the characteristics of the labeled material. (B) Indirect cell labeling methods are strategies for imaging stem cells by inserting a reporter gene into cells through genetic manipulation. The protein expressed by the reporter gene inserted into the stem cell functions as a cell receptor, transporter, enzyme, etc., and has the advantage of being able to image the stem cell permanently and repeatedly *in vivo*. In addition, since the reporter gene is also replicated during the cell division process, the degree of proliferation after stem cell transplantation *in vivo* can be analyzed.

cells transplanted into living organisms in various ways. In this method, labeled cells are explicitly detected *in vivo* and the degree of distribution in target organs can be monitored (14). Images can be taken repeatedly from several hours to several days depending on the half-life of the direct labeling agent or whether it is present in cells. However, since it does not allow imaging of cell proliferation, the imaging signal decreases due to the outflow of the direct labeling agent according to the time lapse (Fig. 1A). Direct cell markers are limited in that they cannot visualize cell activation or cell division. Also, labeled cells can be asymmetrically distributed in progeny cells or lose labeled material during cell division (15).

Optical imaging

Optical imaging is a imaging method acquiring optical signals from contrast agents (16). For optical imaging, a cooled Charge-Coupled Device (CCD) camera is used to reduce thermal noise and improve the sensitivity during imaging (17). Stem cells for fluorescence imaging could be labeled with fluorescent semiconductor nanocrystals such as quantum dots (QDs) or fluorophores (Fig. 2) (18, 19). QDs are semiconductor nanocrystals capable of emitting light at various wavelengths ranging from ultraviolet to near-infrared (NIR) (20). Because QDs have the advantages of high resolution, long duration, high sensitivity, and less toxicity, *in vivo* stem cells were labeled with QDs and imaged. This was demonstrated *in vivo* by labeling stem cells with 6 types of QDs representing various wavelengths (21). Murine embryonic stem (ES) cells were labeled with QD 525, QD 565, QD605, QD 655, QD 705, and QD 800, and 1×10^6 cells were injected subcutaneously into the backs of athymic nude mice. ES cells labeled with QD succeeded in multiplex imaging of ES cells *in vivo* using a single excitation wavelength (465 nm). Such *in vivo* multi-images have great potential for identifying the mobility of stem cells *in vivo*, which is difficult to reproduce *in vitro*, and at the same time identifying the movement of various stem cells. Another study on stem cell imaging using fluorophores showed that the cytoplasmic membrane of mES cells was stained with a DiR dye, a lipophilic NIR fluorescent cyanine dye, and then the stem cells were imaged *in vivo* (22). After labeling mES cells with DiR, 5×10^6 cells were intravenously injected into gastric tumor-bearing mice. The biodistribution of DiR-labeled mES cells was monitored by IVIS imaging within 24 hours. The migration rate of DiR-labeled mES cells to gastric cancer tissue after *in vivo* injection was as fast as 10 minutes and peaked at 2 hours. *Ex vivo* can confirm cell migration to specific organs, but it is not suitable for real-time monitoring. However, monitoring after implantation of stem cell images *in vivo* can identify the accessibility to gastric cancer tissue over time. This shows that DiR-labeled mES cells are applicable to gastric cancer target imaging. In addition, the NIR properties of the DiR dye are suitable for *in vivo* imaging since the autofluorescence of the body itself is reduced at high wavelengths (23). Another study showed that a bone marrow mesenchymal stem cells (BMSCs) was labeled with chloromethyl-benzamide dialkyl carbocyanine-Dil and *in vivo* imaging was acquired to determine whether the stem cells were transplanted to the liver with portal hypertension (24). Other study showed that MSCs were labeled with conjugated polymer based water-dispersible nanoparticles (CPN) and applied to determine the positional information and viability of MSCs *in vitro* and *in vivo* (25). CPN exhibits higher brightness, improved photostability, higher fluorescence quantum yield, and lower cytotoxicity than conventional fluorescent dyes. The resulting fluorescence signal was maintained for 3 weeks after *in vitro* differentiation into osteocytes, adipocytes, and chondrocytes. To analyze the *in vivo* effects of CPN-labeled MSCs on injured site mobility and liver regeneration, an animal model of liver injury was generated by partial hepatectomy in 6-month-old Sprague Dawley rats. CPN-labeled MSCs were injected through the tail vein at 10^6 cells each, and after 3 days, livers were removed and wavelengths for CPN were analyzed. Although this study is not real-time monitoring of MSCs in live animals, it suggests the possibility of safely tracking CPN-labeled MSCs *in vivo*. Further research is needed to determine whether CPN-MSCs migrated to the damaged liver differentiate and affect liver regeneration or function.

Magnetic imaging

The principle of operation of MRIs is that hydrogen nuclei are converted from a rotational motion by a magnetic field. When hydrogen nuclei in the procession state are exposed to electromagnetic waves, only electromagnetic waves that resonate with the precession are emitted. MRI contrast agents contain paramagnetic or superparamagnetic metal ions that affect the MRI signal characteristics of the surrounding tissue and enhance the sensitivity of the MRI. *In vivo* imaging using MRI could be achieved by dosing contrast agents such as superparamagnetic iron-oxide nanoparticles (SPIONs) (Fig. 2). SPIONs treatment of human umbilical cord mesenchymal stem cells (hUC-MSCs) has been reported for non-invasive MRI tracking of stem cells *in vivo* (26). After spinal cord injury (SCI) was induced in rats using a weight drop device, SPIONs-

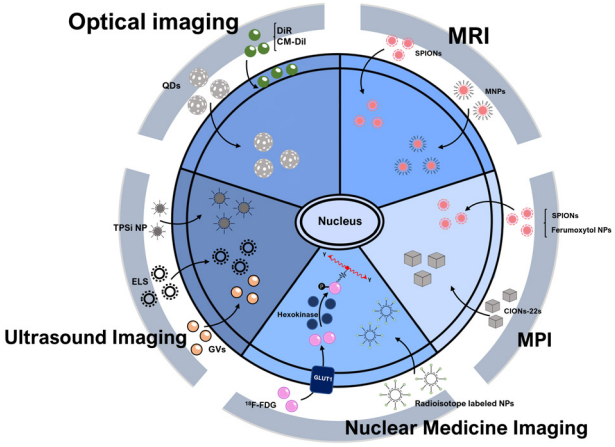

Fig. 2. Principle of direct cell labeling. Principle of direct cell labeling methods is a strategy for imaging stem cells *in vivo* by introducing or labeling direct labeling agents into the body without genetic manipulation. Principle of direct cell labeling methods are relatively simple imaging methods that label stem cells with an agent *in vitro* and then implant them *in vivo*. QDs: quantum dots, CM-DiI: chloromethyl-benzamide dialkyl carbocyanine-DiI, MRI: magnetic resonance imaging, SPIONs: superparamagnetic iron-oxide nanoparticles, MNPs: magnetic nanoparticles, Ferumoxytol NPs: Ferumoxytol nanoparticles, CIONs-22s: cubic iron oxide nanoparticle, MPI: magnetic particle imaging, Radioisotope labeled NPs: Radioisotope labeled nanoparticles, ^{18}F-FDG: 2-deoxy-2-[18F]fluoro-D-glucose, GLUT1: glucose transporter 1, GVs: gas vesicles, ELS: exosome-like silica nanoparticles, TPSi NP: cell-penetrating peptide (virus-1 transactivator of transcription) conjugated porous silicon nanoparticle.

labeled hUC-MSCs were injected into the spinal cord at a concentration of 4×10^4 cells/μl at 2.5 μl. SPIONs-labeled hUC-MSCs injected *in vivo* showed a significant decrease in MRI signal at 1 week and 3 weeks after transplantation. *In vivo*, SPIONs-labeled hUC-MSCs were transplanted into the spinal cord and survival was monitored for at least 8 weeks. This demonstrated that MSCs could survive and migrate in the spinal cord through MRI, and the effect of hUC-MSCs on functional recovery after SCI could be confirmed. It was also demonstrated that dental pulp stem cells (DPSCs) labeled with dextran-coated SPIONs could be successfully monitored by MRI (27). *In vivo* MRI tracking has been reported with SPIONs-labeled BMSCs (28). BMSC transplanted into experimental animals displayed sensitive signals in T2/T2*-weighted images, enabling effective MRI tracking for up to 14 days after transplantation. Fluorescent magnetic nanoparticles (MNPs) has been reported that MSCs were successfully imaged *in vivo* using MNP (29). In a liver cirrhosis mouse model induced by intraperitoneal injection of dimethylnitrosamine (DMN), fluorescent MNP-labeled MSCs (3.0×10^6 cells) were intrasplenicly injected. Then, the viability and mobility of MSCs *in vivo* were monitored using 3-T magnetic resonance equipment. MNP-labeled MSCs demonstrated lower liver-to-muscle noise ratios than those of the pre-injection and non-labeled groups at 3 and 5 hours after transplantation *in vivo*. Therefore, MNP-labeled MSC transplanted by intrasplenic injection in a mouse model of liver lesions by 3-T MRI were successfully mornitered. Through this, it was proved that MNP is suitable for stem cell monitoring through MRI and has mobility and viability *in vivo*. Magneto electroporation (MEP) is a technique based on the mechanism of low voltage pulses, and MEP-labeled MSCs proliferated normally after transplantation, and MRI was successful (30).

Recently, magnetic particle imaging (MPI) have introduced as a new imaging modality with high sensitivity and contrast (31). A study was reported on the dynamic trafficking of SPIONs-labeled MSCs after *in vivo* transplantation through MPI (32). It was demonstrated that the mobility and quantification of labeled MSCs to specific organs could be monitored with MPI. MPI could produce millimeter-scale resolution, high sensitivity, and high contrast angiographic images (33). SPIONs-labeled MSCs (5×10^6 to 8×10^6 cells) were intravenously administered to immunocompetent Fischer 344 rats, and the distribution of MSCs *in vivo* was confirmed by MPI. In this result, it was mornitered that the labeled MSCs were captured in the lung tissue and then removed to the liver within 1 day. MPI-CT imaging revealed that the elimination half-life of MSC iron oxide labels in the liver was 4.6 days, and the *ex vivo* MPI biodistribution of iron was measured in liver, spleen, heart, and lung after injection of labeled MSC. After confirming the distribution of MSCs in several specific organs *ex vivo* through MPI, *in vivo* noninvasive imaging of the labeled MSCs and real-time analysis of quantification provide usefulness. When Ferumoxytol nanoparticles (Ferumoxytol NPs) are labeled on MSC, MPI signals are significantly increased and quantitative information that cannot be obtained by MRI has been collected (34). The cubic iron oxide nanoparticle (CIONs-22s) is a cubic nanoparticle with a 22 nm edge tailored to MPI. It has a much larger saturation magnetization than the existing spherical nanoparticles, so it shows superior performance compared to the existing MPI nanoparticles. BMSCs labeled with CIONs-22 were monitored in real time by MPI regardless of tissue depth and cell location and distribution patterns (35). BMSCs (cell number of ~100,000) labeled with CIONs-22 were administered intravenously to BALB/c mice. MPI over time was then able to accurately track cells over a long period of time,

up to 7 days. This allowed long-term mornitering to examine the overall dynamics of stem cells administered into the body. In addition, when CIONs-22-labeled BMSCs were monitored *in vivo* through MPI, they accumulated in the lungs and migrated to the liver within 3 hours after injection. In this study, MPI succeeded in investigating cell dynamics over time, which could not be confirmed *in vitro/ex vivo*. It suggests the possibility of applying MPI to the accessibility of specific organs for studying stem cell therapy.

Nuclear medicine imaging

PET is a molecular imaging method that monitors positrons induced by radioactive isotopes. Positive charges emitted from radioactive isotopes interact with electrons in the body, generating two 511 KeV photons that are emitted at approximately 180° (36). PET has the advantage of being able to detect even picomolar concentrations, showing very sensitive and quantitative characteristics. For *in vivo* stem cell imaging, it is possible to non-invasively monitor the efficacy of cell-based therapeutics, including stem cell movement, metastasis, survival, and function. However, the half-life and *in vivo* toxicity of the radioactive substances should be considered, as well as the effects of the isotopes on stem cell viability, function, and differentiation (37). Recently, *in vivo* stem cell imaging study has reported with PET after 2-deoxy-2-[18F]fluoro-D-glucose (^{18}F-FDG)-labeled stem cells were transplanted (38-41). In the study, ^{18}F-FDG-labeled MSCs were implanted *in vivo* by various administration methods, and the *in vivo* distribution of the MSCs were analyzed. In this study, MSCs labeled with ^{18}F-FDG were injected into the tail vein of mice (8.5×10^4 cells, 0.1 ml) and rats ($4.6\sim19.0\times10^5$ cells, 1.0 ml). In addition, ^{18}F-FDG-labeled MSCs were injected through rat carotid artery ($4.9\sim16.3\times10^5$ cells, 1.0 ml) and intramyocardial ($1.3\sim1.6\times10^6$ cells, 0.25 ml) injections, and MSC localization was confirmed. It was confirmed that MSCs labeled with ^{18}F-FDG injected through the peripheral vein were entrapped in lung tissue. In addition, ^{18}F-FDG-labeled MSC administration through the carotid artery showed the highest activity in the head, and intramyocardial injection increased the signal from the heart. This study revealed that PET imaging of stem cells using radioactive isotopes varied in signal distribution depending on the stem cell injection route. *In vitro*, pre-labeling of ^{18}F-FDG-labeled MSC is possible, and the uptake of radioactive isotopes can be determined. Furthermore, non-invasive visualization of the distribution of ^{18}F-FDG-labeled MSCs according to various administration modes *in vivo* has the potential to improve the understanding and accessibility of stem cell therapy. Injecting MSCs through the carotid artery may promote recovery of the function of the central nervous system after a brain injury by potentially replacing damaged pericytes associated with MSCs (42). After MSCs were injected into the myocardium, an accumulation of radiotracers near the heart was observed, suggesting that MSCs can potentially be used as a cell-based treatment for diseases such as myocardial infarction. The study not only identified the route of movement of the stem cells *in vivo* but also analyzed their accessibility in specific organs.

The SPECT imaging method is similar to the PET imaging method in that it uses radioactive isotopes, but SPECT uses relatively heavy radioactive isotopes such as ^{99m}TC, ^{123}I, and indium-111 (^{111}In). Protons of SPECT radioactive isotopes combine with electrons in the inner shell to form neutrons and emit electron neutrinos. In this process, electrons from the outer shell are moved to the inner shell for stabilization, and auger electrons and gamma-ray photons are simultaneously generated (43). SPECT have the advantage of being used for relatively long-term *in vivo* imaging. Some stem cells have the ability to aggregate and integrate into tumors when injected into the body. Because of these capabilities, various studies on cell-based anticancer drugs using stem cells are being conducted. One study for *in vivo* stem cell imaging using SPECT showed that luciferase-expressing human adipocyte-derived stem cells (ADSCs) were co-cultured with ^{111}In radiolabelled iron oxide nanoparticles (44). These ADSCs were administered intravenously and intracardiacly to mice with orthotopic breast tumors, and the survival rate of intratumoral ADSCs was measured. As a result, it was demonstrated that more ADSCs implanted *in vivo* by intracardiac administration were present in tumors than by intravenous administration. This is a study that can reveal the accessibility of stem cells to tumors by presenting a simultaneous multiple mornitering method for various imaging means including SPECT. The multimodal imaging approach offers the possibility of analyzing in detail the degree of function, differentiation, and distribution of cells as well as the degree of survival (42). BMSCs labeled with 125I-conjugated nanoparticles were injected into ischemic mouse brains. transplanted BMSCs were imaged through SPECT into the brain, resulting that brain atrophy was reduced, and angiogenesis and neurogenesis were increased to promote nerve recovery. Through this, BMSC has the potential as a treatment for various brain diseases along with the treatment of brain ischemia, which can be continuously mornitered through SPECT.

Ultrasound imaging

Ultrasound imaging is a imaging tool for long-term, non-invasive cell tracking in stem cell-based therapies due to its features of deep penetration and excellent temporal and spatial resolution (45-47). Ultrasound uses Ultrasound Contrast Agents (UCA) to enhance contrast and enhance the echo signal upon detection. In the past, UCAs were micro-sized microbubbles composed of bioinert heavy gases such as lipids, proteins, and biocompatible polymers, but they were limited to large microsizes, poor structural stability, and short half-lives in stem cell tracking (48). Exosome-like silica nanoparticles (ELS) are novel cup-shaped silica nanoparticles and improves biocompatibility in MSCs (49). In addition, since ELS enhances echo generation and ultrasound sensitivity of human mesenchymal stem cell (hMSC) *in vivo*, when ELS-labelled hMSC (1 million) was injected into nude mice, stem cell sensitivity was increased through ultrasound. ELS increases echogenicity *in vitro* and *in vivo* and enables real-time cell tracking/imaging via relatively inexpensive ultrasound. In addition, the ability of ELS to load and release specific drugs has the prospect of improving the viability of stem cells *in vivo* and improving the efficiency of stem cell-based therapy. Cell-penetrating peptide conjugated porous silicon nanoparticle (TPSi NP) improved the viability of labeled cells and the accuracy of stem cell transplantation through a combinational theranostic strategy (50). Intracellular aggregation of TPSi NPs can amplify the coherent scattering of MSCs and thus amplify the ultrasonic signal. The function of TPSi NPs *in vivo* was studied by labeling MSCs and subcutaneously injecting them into nude mice. The ultrasound signal of TPSi NP-labeled MSCs was immediately observed when the number of injected cells *in vivo* was greater than 5×10^4 cells. Clear ultrasound signal amplification of TPSi NP-labeled MSCs can improve the precision of mornitering after stem cell transplantation *in vivo*. Gas vesicles (GVs) are biosynthetic nano-sized particles and perform excellent functions in ultrasound imaging. Recently, GVs were loaded into mouse MSCs and could be imaged *in vivo* in real time using ultrasound imaging (51). *In vivo* ultrasound imaging capability was demonstrated by taking ultrasound images by subcutaneously injecting 1×10^7 cells of GV@MSCs into their lateral malleolus of arthritic rats. GV@MSCs were able to apply real-time ultrasound imaging *in vivo* for 5 days. Bone/cartilage regeneration was induced when GV@MSCs and drugs were co-treated, and there is a possibility of analyzing the distribution and function of MSCs *in vivo* in the future.

Indirect Cell Labeling Methods

Indirect cell labeling methods require genetic manipulation to transplant the reporter gene. Through this, reporter proteins such as cell receptors, transporters, and enzymes are expressed in cells. These proteins promote absorption of radioactive tracers into cells or binding of radioactive tracers to cells, so that specific cells are imaged *in vivo* (Fig. 3). The characteristic of indirect cell labeling methods is that the reporter gene is transmitted during cell division in that genetically engineered cells are used. Through this, long-term imaging is possible by periodically administering the contrast agent. Over time, if the contrast agent is excreted *in vivo* or its function is lost, the imaging signal decreases, but imaging is possible again by re-injecting the contrast agent (Fig. 1B). Reporter gene imaging has the advantage of allowing repetitive "hotspot" imaging at locations within the body following stem cell administration (52). However, indirect cell labeling methods require complex genetic manipulations and

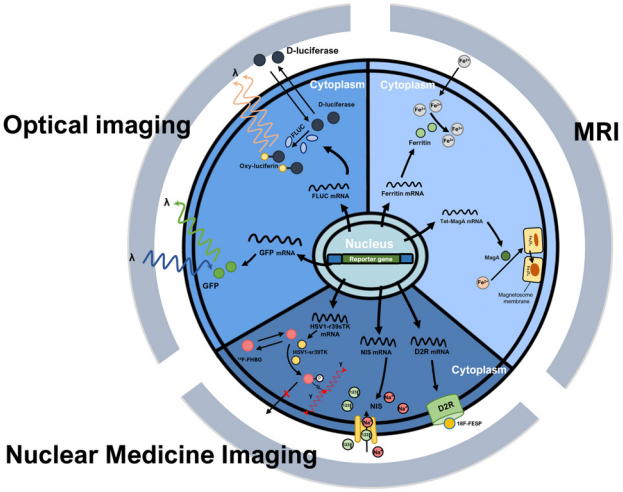

Fig. 3. Principle of indirect cell labeling. Indirect cell labeling methods are methods that permanently detect the survival and proliferation of stem cells *in vivo* through genetic manipulation. There is a method in which the protein expressed by the reporter gene functions as an enzyme and emits a specific wavelength (GFP) and a method in which a contrast agent is additionally administered to the experimental animal (Fluc, D2R, NIS, HSV1-r39sTK). GFP: green fluorescent protein, Fluc: *Photinus pyralis* (firefly) luciferase, Tet: tetracycline, MRI: magnetic resonance imaging, D2R: dopamine 2 receptor, ^{18}F-FESP: 3-(2′-[18F]fluoroethyl) spiperone, NIS: sodium iodide symporter, HSV1-r39sTK: herpes simplex virus 1 thymidine kinase, ^{18}F-FHBG: 9-(4-(18)F-Fluoro-3-[hydroxymethyl]butyl) guanin.

additional stability evaluations.

Optical imaging

Cells expressing fluorescence proteins have been used to confirm protein expression at specific cellular sites and to track specific cell (Fig. 3). Using reporter gene imaging with fluorescent proteins, it is possible to observe the migration and movement of stem cells (53-57). However, fluorescence imaging is limited due to low signal-to-background ratios and autofluorescence (53, 58, 59). Various studies for *in vivo* stem cell imaging are being conducted using fluorescent proteins. One study showed that dynamic tracking of stem cells in an acute liver failure model was successfully achieved using fluorescent dyes in cells (60). In this study, green fluorescent protein (GFP)-expressing ESCs were labeled with a DiR fluorescent dye. Acetaminophen 300 mg/kg was intraperitoneally administered to C57/BL6 male mice to form a liver injury model. Then, 5×10^6 cells of GFP-expressing ESCs labeled with DiR were transplanted into the spleen. ESCs implanted in the spleen *in vivo* were monitored via IVIS. *In vivo* ESCs were trapped inside the spleen 30 minutes after injection into the spleen and gradually moved to the splenic vein over time, and some were detected in the liver 3 hours later. This study presented a method that can evaluate the biodistribution and survival of transplanted cells through a relatively inexpensive method, and can be applied to cell therapy monitoring in that it is an easy-to-use method for experimenters. The cell mobility was analyzed according to the distribution of the fluorescence (61). However, *in vivo* cell imaging using GFP is difficult longer than two weeks after cell transplantation. Luciferases are used as bioluminescent reporters by catalyzing chemical reactions that produce light. Although various types of luciferases exist in nature, of which *Photinus pyralis* (firefly) luciferase (Fluc), *Renilla reniformis* (sea pansy) luciferase (Rluc), and Gaussia princeps (a marine copepod) luciferase (Gluc) have been studied in detail (62). Fluc emits a blue to yellow-green visible light with a wavelength of 490 to 620 nm (63). Since Fluc uses a different substrate than Rluc and Gluc, the production of light is distinct even in the same animal (61). However, the blue bioluminescence of Rluc and Gluc, which has a peak at 480 nm, is strongly absorbed by pigment molecules such as hemoglobin and melanin and has relatively more scatter by tissues, making it less suitable for *in vivo* imaging than Fluc (62). Bioluminescence imaging (BLI) can be also used to measure the expression of a specific protein in a cell and to monitor the transplanted cell *in vivo* (64). BLI is suitable for monitoring cell migration after stem cell transplantation. In one study, after the transplantation of stem cells in a myocardial infarction-induced mouse model using BLI, the cell location and cell survival patterns were analyzed and monitored over time (65). Recently, cell lines expressing luciferase were labeled with a fluorescent dye to analyze the optimal migration route and injection method for MSC migration to the target organ *in vivo* (66). The study evaluated the survival of syngeneic Luc-positive MSCs administered by different routes in non-obese diabetic (NOD) mouse model. The study injected MSCs through various routes, such as intravenous, intrapancreatic, intrasplenic, and subcutaneous. This method of labeling cells for monitoring can confirm the *in vivo* viability of specific cells after transplantation, and the expression of specific genes can be confirmed *ex vivo*. A study on the treatment effect of anaplastic thyroid cancer (ATC) by applying the Tet-On system to MSCs has been reported (67). A doxycycline (DOX)-controlled tetracycline (Tet) inducible system was developed using a retroviral vector expressing herpes simplex virus thymidine kinase (HSV1-sr39TK) with dual reporters (eGFP-Fluc2) in MSCs to develop the Tet-On system. The researchers constructed the MSC-Tet-TK/Fluc2 cell line with the Tet-On system and the MSC-TK/Fluc cell line without the Tet-On system. In an *in vitro* study, ATC (CAL62/Rluc) and engineered MSCs were cultured together, stimulated with DOX, and cell viability was measured according to the presence or absence of the prodrug ganciclovir (GCV). Fluc activity *in vitro* increased in a dose-dependent manner after DOX treatment in MSC-Tet-TK/Fluc cells, and no signal was confirmed in untreated cells. *In vivo*, we investigated the effect of GCV on the survival of MSC-Tet-TK/Fluc and CAK62 induced by DOX. In the left back of a nude mouse, 1.5×10^6 cells of MSC were separately injected in a 1 : 1 ratio with CAL62/Rluc cells. To confirm the decrease in ATC according to the presence or absence of the Tet-On system, 1.5×10^6 cells of MSC-Tet-TK and CAL62/Rluc cells were injected at a ratio of 1 : 1 into the right back of the same mouse. In an *in vivo* experiment, IVIS proved that GCV treatment reduced Rluc activity expressed in CAL62/Rluc when MSC was co-injected with ATC cells (CAL62/Rluc). The results of this study indicated that the MSC's Tet-On/HSV-1-TK/GCV system induced the bystander effect. The suicide gene-based therapy using MSC identified in this study can be suggested as a treatment method for ATC, an aggressive malignant tumor.

MRI

MRI reporter genes contain a specific cellular receptor, an enzyme coding gene, and an endogenous reporter gene

(68). The advantages of this reporter gene are that the signal does not weaken with cell division and the reporter gene is only expressed in viable cells, making it possible to track target cells *in vivo* indefinitely. With stem cell transplantation, it might be possible to alleviate many diseases, such as cardiovascular disorders, brain injuries, multiple sclerosis, urinary system diseases, cartilage lesions, and diabetes. Additionally, the reporter gene can be inserted under a specific promoter that is activated only when the stem cells differentiate into a specific phenotype, enabling specialized stem cell imaging to be implemented on a micro-scale (69). MRI reporter genes can be classified into three classes based on the types of encoded genes: reporter genes encoding an enzyme, such as tyrosinase and β-galactosidase; reporter genes encoding a receptor on the cell, such as transferrin receptor; and endogenous reporter genes, such as the ferritin reporter gene (70). Transferrin receptor and ferritin reporter genes are iron-based reporter genes. Various studies in MRI have demonstrated that the co-expression of ferritin and transferrin receptors of neural stem cells show signal loss in iron-rich environments (71-77). Tyrosinase and β-galactosidase are commonly used enzyme-based reporter genes for MRIs (71). The overexpression of human tyrosinase induces higher metal binding, which may result in enhanced MRI signal intensity. Additionally, MRIs based on the ferritin reporter gene can be used to trace the tendency of MSCs to accumulate in gliomas *in vivo* (78, 79). MSCs into which the reporter gene ferritin heavy chain (FTH1) was introduced were subcutaneously inoculated into nude mice, and signal changes in xenografts were observed through MRI *in vivo*. This study is a successful case of stem cell imaging *in vivo* through the change in T2 value after transduction of an MRI reporter gene into MSCs. And by developing a new MRI model based on FTH1 reporter gene expression, it is possible to more sensitively detect the occurrence of malignant transformation of MSCs. Stem cell mornitering *in vivo* has been studied by regulating MagA, a gene involved in iron transport and formation of forming magnetite (Fe_3O_4) crystals, through the Tet-On system (80). An mESC-MagA cell line was established through lentivirus transduction of Tet-MagA into mESC. Severe combined immune-deficient (SCID) mice were implanted by stereotactic injection with 1×10^5 cells of mESC-MagA and mESC-wild type, respectively, treated with Dox (1 μg/ml) and ferric citrate (25 μM) for 3 days. Through this experiment, we tried to monitor the suitability of mESC-MagA and mESC-wild type for 7T MRI in induced "ON" and non-induced "OFF" conditions *in vivo*. As a result, significant changes were shown in the transverse relaxation rate (R2 or 1/T2) and susceptibility weighted MRI contrast in the mESC-MagA cell line. Intracranial mESC-MagA grafts produced sufficient T2 and susceptibility weighted contrast at 7T. When DOX was injected into mice transplanted with mESC-MagA through diet, the presence of cells *in vivo* could be monitored through MRI. Based on these results, cells expressing MagA that can be controlled by the Tet-On system can be monitored non-invasively *in vivo*, and the status of repeated cell transplantation can be evaluated over a long period of time through repeated intake of ferric citrate and DOX. It was analyzed that the expression of MagA does not affect the function of mESCs at the *in vitro* level. *In vivo*, it was determined whether MagA expression in actual experimental animals was suitable for MRI and controllable imaging through the Tet-On system. The Tet-On induction system has the advantage of reducing the continuous accumulation of MagA and iron *in vivo* because it can inhibit the necessary expression of MagA. In view of these advantages, *in vivo* cell transplantation for stem cell-based therapy can be monitored only at a specific time point, which shows the possibility of reducing the burden of the body due to the accumulation of contrast agents *in vivo*.

Nuclear medicine imaging

For nuclear medicine imaging, there are various *in vivo* reporter gene in PET and SPECT imaging (81). Among the PET reporter genes, herpes simplex virus 1 thymidine kinase (HSV1-tk) is used for *in vivo* imaging using a substrate with a radioactive isotope such as 9-(4-(18)F-Fluoro-3-[hydroxymethyl]butyl)guanin (^{18}F-FHBG) or ^{124}I-FIAU (82, 83). Dopamine 2 receptor (D2R) is a protein expressed in the human striatum and pituitary and is a PET reporter gene that specifically pairs with radiolabeled compounds, such as 3-(2'-[^{18}F]fluoroethyl)spiperone (^{18}F-FESP) (84, 85). One study was conducted on whether D2R was suitable for non-invasive real-time imaging of stem cells *in vivo* by transplanting hMSC (86). The study succeeded in using D2R-overexpressing hMSC *in vivo* for imaging by utilizing the high sensitivity and high spatial resolution of the PET reporter gene system. *In vitro*, it was confirmed that the stem cell characteristics of hMSC were not changed by D2R, and *in vivo*, D2R-overexpressing hMSC (2.4×10^7 cells) was injected into the muscle of the hind limb of athymic nude rats. After transplantation, 20 MBq of 18F-fallypride was intravenously injected and morniter-ing was performed through PET. Specific signals *in vivo* were detected at the transplant site up to 7 days. Through this, the application period of D2R for periodic radioactive isotope injection and the location of hMSC relative to the injection site after cell labeling were confirmed *in*

Table 1. Imaging techniques for stem cell labeling

Goal	Strategy	Imaging modality	Labeling strategy	Cell type	Cells volume	Animals	Reference
Early cell localization and homing	Direct cell labeling methods	Optical imaging	QDs	Murine ESCs	1×10^6	Athymic nude mice	(20, 21)
			Fluorophores	Murine ESCs	5×10^6	Gastric tumor-bearing mice	(22-24)
			CPN	MSCs	1×10^6	Sprague Dawley rats	(25)
		Magnetic imaging	SPIONs	Human umbilical cord MSCs	1×10^6	SCI induced rats	(26-28)
			Fluorescent magnetic nanoparticles	MSCs	3×10^6	Liver cirrhosis mouse	(29)
			Magneto electroporation	BMSCs	$\sim1\times10^6$	BALB/cmice	(30)
		Magnetic particle imaging	SPIONs	MSCs	5×10^6 $\sim8\times10^6$	Fischer 344 rats	(32)
			Ferumoxytol nanoparticles	MSCs	1×10^6	C57B1/6 mice	(34)
			CIONs-22s	BMSCs	$\sim1\times10^6$	BALB/cmice	(35)
		Nuclear medicine imaging	^{18}F-FDG	MSCs	8.5×10^4	C57BL/6 mouse Wistar rats	(38-41)
			Indium-111 radiolabelledIron oxide nanoparticles	Adipocyte-derived stem cells	1×10^5	NSG mice	(44)
		Ultrasound imaging	ELS	hMSCs	1×10^7	Nude mice	(49)
			TPSi NP	MSCs	1×10^6	BALB/c nude mice	(50)
			GVs	Mouse MSCs	1×10^7	Arthritic rats	(51)
Long term monitering of cell viability	Indirect cell labeling methods	Optical imaging	GFP	ESCs	5×10^6	C57BL/6 mouse	(61)
			Fluc	MSCs	5×10^5	FVB mice	(65)
		MRI	Ferritin	MSCs	2×10^6	Wistar rats	(77)
		Nuclear medicine imaging	D2R	hMSCs	2.4×10^7	Arthritic nude rats	(84)
			NIS	MSCs	1×10^6	Athymic nude mice	(88, 89, 90-93)

Labeling strategy for *in vivo* imaging methods is various depending on cell type, cell volume, animals and so on.
QDs: quantum dots, ESCs: embryonic stem cells, CPN: conjugated polymer based water-dispersible nanoparticles, MSCs: mesenchymal stem cells, SPIONs: superparamagnetic iron-oxide nanoparticles, SCI: spinal cord injury, BMSCs: bone marrow mesenchymal stem cells, CIONs-22s: cubic iron oxide nanoparticle, ^{18}F-FDG: 2-deoxy-2-[18F]fluoro-D-glucose, NSG: non-obese diabetic/severe combined immunodeficiency/gamma, ELS: exosome-like silica nanoparticles, hMSCs: human mesenchymal stem cells, TPSi NP: cell-penetrating peptide (virus-1 transactivator of transcription) conjugated porous silicon nanoparticle, GVs: gas vesicles, GFP: green fluorescent protein, Fluc: *Photinus pyralis* (firefly) luciferase, MRI: magnetic resonance imaging, D2R: dopamine 2 receptor, NIS: sodium iodide symporter.

vivo. The sodium iodide symporter (NIS) reporter gene is a glycoprotein located in the basolateral membrane, which actively transports iodide (87, 88). The NIS introduces various radionuclides such as ^{131}I, ^{123}I, ^{125}I, ^{124}I, ^{99m}Tc, and ^{188}Re into cells according to the purpose (89). The expression of NIS in stem cells could evaluate the survival rate and mobility of stem cells after transplantation *in vivo*, such as the transplantation of cardiac stem cells and the migration of MSCs to the breast cancer tumor stroma (90, 91). Since NIS is a non-immunogenic protein, it is an optimal reporter gene and gene therapy candidate. In addition, NIS can symport the radiotracer ^{99m}Tc-pertechnetate ($^{99m}TcO4^-$) for SPECT. Various NIS-expressing cells were imaged and monitored using $^{99m}TcO4^-$ *in vivo* (92, 93). NIS is also used as a therapeutic gene in research for stem cell therapy. MSCs that expressed NIS were used to image tumors through the recruitment of the MSCs to the tumor (94, 95).

Conclusion

This review described various methods for *in vivo* stem cell imaging (Table 1). Through direct and indirect labeling methods, the transplanted stem cell could be labeled and monitored in optical imaging, MRI, ultrasound, PET, and SPECT. Research on stem cells as a cell-based treatment and their clinical applications is ongoing. Future imaging technologies have the potential to monitor specific stem cells with high sensitivity and high resolution. In the future, more precise and complex *in vivo* cell imaging methods could be developed. Through this, new research directions for incurable diseases or previously unexplored fields may be presented.

ORCID

Seongje Hong, https://orcid.org/0009-0007-0711-144X
Dong-Sung Lee, https://orcid.org/0000-0003-3815-7057
Geun-Woo Bae, https://orcid.org/0009-0000-7887-3694
Juhyeong Jeon, https://orcid.org/0009-0007-1860-5197
Hak Kyun Kim, https://orcid.org/0000-0002-7709-7870
Siyeon Rhee, https://orcid.org/0000-0002-7642-4016
Kyung Oh Jung, https://orcid.org/0000-0002-5000-7791

Funding

This research was supported by the Chung-Ang University Research Grants in 2021 to KOJ. This research was also supported by 2022 Advanced Facility Fund of the University of Seoul to DSL.

Potential Conflict of Interest

There is no potential conflict of interest to declare.

Authors' Contribution

Conceptualization: SH, KOJ. Data curation: SH, KOJ. Formal analysis: SH, GWB, JJ, SR. Funding acquisition: DSL, KOJ. Investigation: SH, GWB, JJ. Methodology: SH, GWB, JJ. Project administration: DSL, SR, HKK, KOJ. Resources: SH, GWB, JJ. Software: SH, GWB, JJ. Supervision: DSL, KOJ. Validation: DSL, SR, HKK, KOJ. Visualization: SH, KOJ. Writing – original draft: SH, GWB, JJ, KOJ. Writing – review and editing: SH, DSL, SR, HKK, KOJ.

References

1. Mason C, Dunnill P. A brief definition of regenerative medicine. Regen Med 2008;3:1-5
2. Mahla RS. Stem cells applications in regenerative medicine and disease therapeutics. Int J Cell Biol 2016;2016:6940283
3. Leferink AM, Chng YC, van Blitterswijk CA, Moroni L. Distribution and viability of fetal and adult human bone marrow stromal cells in a biaxial rotating vessel bioreactor after seeding on polymeric 3D additive manufactured scaffolds. Front Bioeng Biotechnol 2015;3:169
4. Gubareva EA, Sjöqvist S, Gilevich IV, et al. Orthotopic transplantation of a tissue engineered diaphragm in rats. Biomaterials 2016;77:320-335
5. Garzón I, Pérez-Köhler B, Garrido-Gómez J, et al. Evaluation of the cell viability of human Wharton's jelly stem cells for use in cell therapy. Tissue Eng Part C Methods 2012;18:408-419
6. Thompson PA, Perera T, Marin D, et al. Double umbilical cord blood transplant is effective therapy for relapsed or refractory Hodgkin lymphoma. Leuk Lymphoma 2016;57:1607-1615
7. Boehm-Sturm P, Mengler L, Wecker S, Hoehn M, Kallur T. In vivo tracking of human neural stem cells with 19F magnetic resonance imaging. PLoS One 2011;6:e29040
8. Hong H, Yang Y, Zhang Y, Cai W. Non-invasive cell tracking in cancer and cancer therapy. Curr Top Med Chem 2010;10:1237-1248
9. Wang L, Maslov K, Wang LV. Single-cell label-free photoacoustic flowoxigraphy in vivo. Proc Natl Acad Sci U S A 2013;110:5759-5764
10. Murakami T, Chun N. Bioluminescent imaging and organ-specific metastasis of human cancer cells [Internet]. Bellingham: The International Society for Optics and Photonics (SPIE); 2009 Dec 17 [cited 2023 Jun 1]. Available from: https://spie.org/news/2501-bioluminescent-imaging-and-organ-specific-metastasis-of-human-cancer-cells?SSO=1
11. Iwano S, Sugiyama M, Hama H, et al. Single-cell bioluminescence imaging of deep tissue in freely moving animals. Science 2018;359:935-939
12. Herynek V, Turnovcová K, Gálisová A, et al. Manganese-

zinc ferrites: safe and efficient nanolabels for cell imaging and tracking in vivo. ChemistryOpen 2019;8:155-165
13. Man F, Lim L, Volpe A, et al. In vivo PET tracking of ^{89}Zr-Labeled Vγ9Vδ2 T cells to mouse xenograft breast tumors activated with liposomal alendronate. Mol Ther 2019;27:219-229
14. Kircher MF, Gambhir SS, Grimm J. Noninvasive cell-tracking methods. Nat Rev Clin Oncol 2011;8:677-688
15. Youn H, Hong KJ. In vivo non invasive molecular imaging for immune cell tracking in small animals. Immune Netw 2012;12:223-229
16. Concilio SC, Russell SJ, Peng KW. A brief review of reporter gene imaging in oncolytic virotherapy and gene therapy. Mol Ther Oncolytics 2021;21:98-109
17. Martelli C, Lo Dico A, Diceglie C, Lucignani G, Ottobrini L. Optical imaging probes in oncology. Oncotarget 2016;7: 48753-48787
18. Michalet X, Pinaud FF, Bentolila LA, et al. Quantum dots for live cells, *in vivo* imaging, and diagnostics. Science 2005;307:538-544
19. Kalchenko V, Shivtiel S, Malina V, et al. Use of lipophilic near-infrared dye in whole-body optical imaging of hematopoietic cell homing. J Biomed Opt 2006;11:050507
20. Seleverstov O, Zabirnyk O, Zscharnack M, et al. Quantum dots for human mesenchymal stem cells labeling. A size-dependent autophagy activation. Nano Lett 2006;6:2826-2832
21. Lin S, Xie X, Patel MR, et al. Quantum dot imaging for embryonic stem cells. BMC Biotechnol 2007;7:67
22. Ruan J, Song H, Li C, et al. DiR-labeled embryonic stem cells for targeted imaging of *in vivo* gastric cancer cells. Theranostics 2012;2:618-628
23. Lassailly F, Griessinger E, Bonnet D. "Microenvironmental contaminations" induced by fluorescent lipophilic dyes used for noninvasive *in vitro* and *in vivo* cell tracking. Blood 2010;115:5347-5354
24. Sun S, Chen G, Xu M, Qiao Y, Zheng S. Differentiation and migration of bone marrow mesenchymal stem cells transplanted through the spleen in rats with portal hypertension. PLoS One 2013;8:e83523.
25. Akhan E, Tuncel D, Akcali KC. Nanoparticle labeling of bone marrow-derived rat mesenchymal stem cells: their use in differentiation and tracking. Biomed Res Int 2015;2015: 298430
26. Hu SL, Lu PG, Zhang LJ, et al. In vivo magnetic resonance imaging tracking of SPIO-labeled human umbilical cord mesenchymal stem cells. J Cell Biochem 2012;113:1005-1012
27. Zare S, Mehrabani D, Jalli R, et al. MRI-tracking of dental pulp stem cells in vitro and in vivo using dextran-coated superparamagnetic iron oxide nanoparticles. J Clin Med 2019;8:1418
28. Pang P, Wu C, Gong F, et al. Nanovector for gene transfection and MR imaging of mesenchymal stem cells. J Biomed Nanotechnol 2015;11:644-656
29. Kim TH, Kim JK, Shim W, Kim SY, Park TJ, Jung JY. Tracking of transplanted mesenchymal stem cells labeled with fluorescent magnetic nanoparticle in liver cirrhosis rat model with 3-T MRI. Magn Reson Imaging 2010;28:1004-1013
30. Walczak P, Kedziorek DA, Gilad AA, Lin S, Bulte JW. Instant MR labeling of stem cells using magnetoelectroporation. Magn Reson Med 2005;54:769-774
31. Zhou XY, Tay ZW, Chandrasekharan P, et al. Magnetic particle imaging for radiation-free, sensitive and high-contrast vascular imaging and cell tracking. Curr Opin Chem Biol 2018;45:131-138
32. Du Y, Lai PT, Leung CH, Pong PW. Design of superparamagnetic nanoparticles for magnetic particle imaging (MPI). Int J Mol Sci 2013;14:18682-18710
33. Zheng B, von See MP, Yu E, et al. Quantitative magnetic particle imaging monitors the transplantation, biodistribution, and clearance of stem cells in vivo. Theranostics 2016;6:291-301
34. Sehl OC, Makela AV, Hamilton AM, Foster PJ. Trimodal cell tracking in vivo: combining iron- and fluorine-based magnetic resonance imaging with magnetic particle imaging to monitor the delivery of mesenchymal stem cells and the ensuing inflammation. Tomography 2019;5:367-376
35. Wang Q, Ma X, Liao H, et al. Artificially engineered cubic iron oxide nanoparticle as a high-performance magnetic particle imaging tracer for stem cell tracking. ACS Nano 2020;14:2053-2062
36. Uenomachi M, Takahashi M, Shimazoe K, et al. Simultaneous in vivo imaging with PET and SPECT tracers using a Compton-PET hybrid camera. Sci Rep 2021;11:17933
37. Tong L, Zhao H, He Z, Li Z. Current perspectives on molecular imaging for tracking stem cell therapy. In: Erondu OF, editor. Medical Imaging in Clinical Practice. InTech; 2013. 63-79
38. Jiang W, Chalich Y, Deen MJ. Sensors for positron emission tomography applications. Sensors (Basel) 2019;19:5019
39. Kapoor V, McCook BM, Torok FS. An introduction to PET-CT imaging. Radiographics 2004;24:523-543
40. Cook GJ, Wegner EA, Fogelman I. Pitfalls and artifacts in 18FDG PET and PET/CT oncologic imaging. Semin Nucl Med 2004;34:122-133
41. Nose N, Nogami S, Koshino K, et al. [18F]FDG-labelled stem cell PET imaging in different route of administrations and multiple animal species. Sci Rep 2021;11:10896
42. Yao M, Shi X, Zuo C, et al. Engineering of SPECT/photoacoustic imaging/antioxidative stress triple-function nanoprobe for advanced mesenchymal stem cell therapy of cerebral ischemia. ACS Appl Mater Interfaces 2020;12:37885-37895
43. Wang J, Jokerst JV. Stem cell imaging: tools to improve cell delivery and viability. Stem Cells Int 2016;2016:9240652
44. Zaw Thin M, Allan H, Bofinger R, et al. Multi-modal imaging probe for assessing the efficiency of stem cell delivery to orthotopic breast tumours. Nanoscale 2020;12:16570-16585
45. Chen F, Jokerst JV. Stem cell tracking with nanoparticle-based ultrasound contrast agents. Methods Mol Biol 2020;

2126:141-153
46. Abou-Elkacem L, Bachawal SV, Willmann JK. Ultrasound molecular imaging: moving toward clinical translation. Eur J Radiol 2015;84:1685-1693
47. James ML, Gambhir SS. A molecular imaging primer: modalities, imaging agents, and applications. Physiol Rev 2012;92:897-965
48. Xu C, Feng Q, Ning P, Li Z, Qin Y, Cheng Y. Recent advances on nanoparticle-based imaging contrast agents for in vivo stem cell tracking. Mat Matters 2021;16:2
49. Chen F, Ma M, Wang J, et al. Exosome-like silica nanoparticles: a novel ultrasound contrast agent for stem cell imaging. Nanoscale 2017;9:402-411
50. Qi S, Zhang P, Ma M, et al. Cellular internalization-induced aggregation of porous silicon nanoparticles for ultrasound imaging and protein-mediated protection of stem cells. Small 2019;15:e1804332
51. Gong Z, He Y, Zhou M, et al. Ultrasound imaging tracking of mesenchymal stem cells intracellularly labeled with biosynthetic gas vesicles for treatment of rheumatoid arthritis. Theranostics 2022;12:2370-2382
52. Gawne PJ, Man F, Blower PJ, T M de Rosales R. Direct cell radiolabeling for *in vivo* cell tracking with PET and SPECT imaging. Chem Rev 2022;122:10266-10318
53. Kang JH, Chung JK. Molecular-genetic imaging based on reporter gene expression. J Nucl Med 2008;49 Suppl 2: 164S-179S
54. Müller-Taubenberger A. Application of fluorescent protein tags as reporters in live-cell imaging studies. Methods Mol Biol 2006;346:229-246
55. Chudakov DM, Lukyanov S, Lukyanov KA. Fluorescent proteins as a toolkit for in vivo imaging. Trends Biotechnol 2005;23:605-613
56. Ke CC, Liu RS, Suetsugu A, et al. In vivo fluorescence imaging reveals the promotion of mammary tumorigenesis by mesenchymal stromal cells. PLoS One 2013;8:e69658
57. Chen Q, Wang X, Wu H, et al. Establishment of a dual-color fluorescence tracing orthotopic transplantation model of hepatocellular carcinoma. Mol Med Rep 2016;13:762-768
58. Troy T, Jekic-McMullen D, Sambucetti L, Rice B. Quantitative comparison of the sensitivity of detection of fluorescent and bioluminescent reporters in animal models. Mol Imaging 2004;3:9-23
59. Hoffman RM. Application of GFP imaging in cancer. Lab Invest 2015;95:432-452
60. Ezzat T, Dhar DK, Malago M, Olde Damink SW. Dynamic tracking of stem cells in an acute liver failure model. World J Gastroenterol 2012;18:507-516
61. Bhaumik S, Lewis XZ, Gambhir SS. Optical imaging of Renilla luciferase, synthetic Renilla luciferase, and firefly luciferase reporter gene expression in living mice. J Biomed Opt 2004;9:578-586
62. Badr CE, Tannous BA. Bioluminescence imaging: progress and applications. Trends Biotechnol 2011;29:624-633
63. Iyer M, Sato M, Johnson M, Gambhir SS, Wu L. Applications of molecular imaging in cancer gene therapy. Curr Gene Ther 2005;5:607-618
64. Subramaniam D, Natarajan G, Ramalingam S, et al. Translation inhibition during cell cycle arrest and apoptosis: Mcl-1 is a novel target for RNA binding protein CUGBP2. Am J Physiol Gastrointest Liver Physiol 2008;294:G1025-G1032
65. van der Bogt KE, Sheikh AY, Schrepfer S, et al. Comparison of different adult stem cell types for treatment of myocardial ischemia. Circulation 2008;118(14 Suppl):S121-S129
66. Preda MB, Neculachi CA, Fenyo IM, et al. Short lifespan of syngeneic transplanted MSC is a consequence of in vivo apoptosis and immune cell recruitment in mice. Cell Death Dis 2021;12:566
67. Kalimuthu S, Oh JM, Gangadaran P, et al. Genetically engineered suicide gene in mesenchymal stem cells using a Tet-On system for anaplastic thyroid cancer. PLoS One 2017;12:e0181318
68. Gao T, Wang P, Gong T, et al. Reporter genes for brain imaging using MRI, SPECT and PET. Int J Mol Sci 2022;23:8443
69. Kraitchman DL, Bulte JW. Imaging of stem cells using MRI. Basic Res Cardiol 2008;103:105-113
70. Yang C, Tian R, Liu T, Liu G. MRI reporter genes for noninvasive molecular imaging. Molecules 2016;21:580
71. Gilad AA, Ziv K, McMahon MT, van Zijl PC, Neeman M, Bulte JW. MRI reporter genes. J Nucl Med 2008;49: 1905-1908
72. Weissleder R, Moore A, Mahmood U, et al. In vivo magnetic resonance imaging of transgene expression. Nat Med 2000;6:351-354
73. Ichikawa T, Högemann D, Saeki Y, et al. MRI of transgene expression: correlation to therapeutic gene expression. Neoplasia 2002;4:523-530
74. Cohen B, Dafni H, Meir G, Harmelin A, Neeman M. Ferritin as an endogenous MRI reporter for noninvasive imaging of gene expression in C6 glioma tumors. Neoplasia 2005;7:109-117
75. Cohen B, Ziv K, Plaks V, et al. MRI detection of transcriptional regulation of gene expression in transgenic mice. Nat Med 2007;13:498-503
76. Genove G, DeMarco U, Xu H, Goins WF, Ahrens ET. A new transgene reporter for in vivo magnetic resonance imaging. Nat Med 2005;11:450-454
77. Deans AE, Wadghiri YZ, Bernas LM, Yu X, Rutt BK, Turnbull DH. Cellular MRI contrast via coexpression of transferrin receptor and ferritin. Magn Reson Med 2006; 56:51-59
78. Cao M, Mao J, Duan X, et al. In vivo tracking of the tropism of mesenchymal stem cells to malignant gliomas using reporter gene-based MR imaging. Int J Cancer 2018;142: 1033-1046
79. Sun J, Huang J, Bao G, et al. MRI detection of the malignant transformation of stem cells through reporter gene expression driven by a tumor-specific promoter. Stem Cell Res Ther 2021;12:284

80. Cho IK, Moran SP, Paudyal R, et al. Longitudinal monitoring of stem cell grafts in vivo using magnetic resonance imaging with inducible maga as a genetic reporter. Theranostics 2014;4:972-989
81. Gambhir SS. Molecular imaging of cancer with positron emission tomography. Nat Rev Cancer 2002;2:683-693
82. Youn H, Hong KJ. In vivo noninvasive small animal molecular imaging. Osong Public Health Res Perspect 2012;3: 48-59
83. Tjuvajev JG, Doubrovin M, Akhurst T, et al. Comparison of radiolabeled nucleoside probes (FIAU, FHBG, and FHPG) for PET imaging of HSV1-tk gene expression. J Nucl Med 2002;43:1072-1083
84. Peñuelas I, Haberkorn U, Yaghoubi S, Gambhir SS. Gene therapy imaging in patients for oncological applications. Eur J Nucl Med Mol Imaging. 2005;32 Suppl 2:S384-S403
85. Liang Q, Satyamurthy N, Barrio JR, et al. Noninvasive, quantitative imaging in living animals of a mutant dopamine D2 receptor reporter gene in which ligand binding is uncoupled from signal transduction. Gene Ther 2001;8: 1490-1498
86. Schönitzer V, Haasters F, Käsbauer S, et al. In vivo mesenchymal stem cell tracking with PET using the dopamine type 2 receptor and 18F-fallypride. J Nucl Med 2014;55: 1342-1347
87. Kitzberger C, Spellerberg R, Morath V, et al. The sodium iodide symporter (NIS) as theranostic gene: its emerging role in new imaging modalities and non-viral gene therapy. EJNMMI Res 2022;12:25
88. Spitzweg C, Bible KC, Hofbauer LC, Morris JC. Advanced radioiodine-refractory differentiated thyroid cancer: the sodium iodide symporter and other emerging therapeutic targets. Lancet Diabetes Endocrinol 2014;2:830-842
89. Gu E, Chen WY, Gu J, Burridge P, Wu JC. Molecular imaging of stem cells: tracking survival, biodistribution, tumorigenicity, and immunogenicity. Theranostics 2012;2: 335-345
90. Terrovitis J, Kwok KF, Lautamäki R, et al. Ectopic expression of the sodium-iodide symporter enables imaging of transplanted cardiac stem cells in vivo by single-photon emission computed tomography or positron emission tomography. J Am Coll Cardiol 2008;52:1652-1660
91. Dwyer RM, Ryan J, Havelin RJ, et al. Mesenchymal Stem Cell-mediated delivery of the sodium iodide symporter supports radionuclide imaging and treatment of breast cancer. Stem Cells 2011;29:1149-1157
92. Sharif-Paghaleh E, Sunassee K, Tavaré R, et al. In vivo SPECT reporter gene imaging of regulatory T cells. PLoS One 2011;6:e25857
93. Price DN, McBride AA, Anton M, et al. Longitudinal assessment of lung cancer progression in mice using the sodium iodide symporter reporter gene and SPECT/CT imaging. PLoS One 2016;11:e0169107
94. Knoop K, Kolokythas M, Klutz K, et al. Image-guided, tumor stroma-targeted 131I therapy of hepatocellular cancer after systemic mesenchymal stem cell-mediated NIS gene delivery. Mol Ther 2011;19:1704-1713
95. Conrad C, Hüsemann Y, Niess H, et al. Linking transgene expression of engineered mesenchymal stem cells and angiopoietin-1-induced differentiation to target cancer angiogenesis. Ann Surg 2011;253:566-571